

Transcriptomic analysis identifies genes and pathways related to myrmecophagy in the Malayan pangolin

Jing E Ma¹, Lin Miao Li¹, Hai Ying Jiang¹, Xiu Juan Zhang¹, Juan Eyre^{Corresp.}¹, Guan Yu Li¹, Li Hong Yuan¹, Jun Wu², Jin Ping Chen^{Corresp.}³

¹ Guangdong Key Laboratory of Animal Conservation and Resource Utilization, Guangdong Institute of Applied Biological Resources, Guangzhou, Guangdong, China

² Wildlife disease surveillance and molecular ecology research Center, Nanjing Institute of Environmental Sciences under Ministry of Environmental Protection, Guangzhou, Guangdong, China

³ xingangxi, Guangdong Institute of Applied Biological Resources, Guangzhou, Guangdong, China

Corresponding Authors: Juan Eyre, Jin Ping Chen

Email address: lijuan315@mailsucas.ac.cn, chenjp@gdei.gd.cn

The Malayan pangolin, an unusual mammal that is a scale-covered, toothless specialist myrmecophage, is maintained primarily through captive breeding in China. Maintaining this species in captivity is a significant challenge partly because little known of the molecular mechanisms on its digestive system up till now. Here, the first large-scale sequencing analysis of transcriptomes from salivary glands, liver and small intestine with Malayan pangolin genome was performed, compared with published data sets involving liver transcriptome profiles from a pregnant Malayan pangolin. A total of 24,452 transcripts were obtained, among which 22,538 transcripts were annotated on the basis of seven databases. In addition, 3,373 new genes were predicted, of which 1,459 were annotated. Several pathways were found to be involved in myrmecophagy, including olfactory transduction, amino sugar and nucleotide sugar metabolism, lipid metabolism, and terpenoid and polyketide metabolism pathways. Several of the annotated transcripts were involved in digestive functions: 997 transcripts were related to sensory perception, 129 transcripts belonged to digestive enzyme gene families, and 199 transcripts were related to molecular transporters. One transcript of acidic mammalian chitinase was found in the annotated data, and these might be closely related to the unique digestive function of pangolins. These pathways and transcripts are involved in specialization processes related to myrmecophagy and carbohydrate, protein and lipid digestive pathways, thus probably reflecting adaptations to myrmecophage. Our study has firstly revealed the molecular mechanism of myrmecophagy in Malayan pangolin that may play a role in the protection of the pangolin.

24

25 **Abstract**

26 The Malayan pangolin (*Manis javanica*), an unusual mammal that is a scale-covered,
27 toothless specialist myrmecophage, is maintained primarily through captive breeding in China.
28 Maintaining this species in captivity is a significant challenge partly because little known of the
29 molecular mechanisms on its digestive system up till now. Here, the first large-scale sequencing
30 analysis of transcriptomes from salivary glands, liver and small intestine with *M. javanica* genome
31 was performed, compared with published data sets involving liver transcriptome profiles from a
32 pregnant *M. javanica*. A total of 24,452 transcripts were obtained, among which 22,538 transcripts
33 were annotated on the basis of seven databases. In addition, 3,373 new genes were predicted, of
34 which 1,459 were annotated. Several pathways were found to be involved in myrmecophagy,
35 including olfactory transduction, amino sugar and nucleotide sugar metabolism, lipid metabolism,
36 and terpenoid and polyketide metabolism pathways. Several of the annotated transcripts were
37 involved in digestive functions: 997 transcripts were related to sensory perception, 129 transcripts
38 belonged to digestive enzyme gene families, and 199 transcripts were related to molecular
39 transporters. One transcript of acidic mammalian chitinase was found in the annotated data, and
40 these might be closely related to the unique digestive function of pangolins. These pathways and
41 transcripts are involved in specialization processes related to myrmecophagy (insectivory) and
42 carbohydrate, protein and lipid digestive pathways, thus probably reflecting adaptations to
43 myrmecophage. Our study has firstly revealed the molecular mechanism of myrmecophagy in *M.*
44 *javanica* that may play a role in the protection of the pangolin.

45 **Keywords:** pangolin, conservation, digestion, myrmecophagy.

46

47 **Introduction**

48 Pangolins, also known as scaly anteaters, are eutherians and unique placental mammals. Eight
49 pangolin species are recognized: four from Asia, *M. javanica*, *M. pentadactyla*, *M. crassicaudata*,
50 and *M. culionensis*, and four from Africa, *M. tricuspis*, *M. tetradactyla*, *M. gigantea*, and *M.*
51 *temminckii* (Choo et al. 2016). *M. javanica* is found mainly in Southeast Asia (Trageser et al.
52 2017). In pangolins, unlike other placental mammals, the skin is covered by large and overlapping
53 keratinized scales (Meyer et al. 2013). Furthermore, pangolins are edentulous or toothless and are
54 thus specialized within an already unusual mammalian dietary niche (Pietersen et al. 2015; Yang
55 et al. 2007). Pangolins have been reported to consume four kinds of ants (*Anoplolepis*
56 *steingroeveri*, *Camponotus fulvopilosus*, and two *Crematogaster spp.*) and one kind of termite
57 species (*Trinervitermes trinervoides*) (Pietersen et al. 2015). They also have a well-developed
58 muscular system for fossorial or arboreal behavior and a remarkable olfactory system. As predators
59 of ants and termites, pangolins have a specialized diet and perform an important ecological role in
60 regulating insect populations. Individual adult pangolins have been estimated to consume more
61 than 70 million insects annually and have a significant effect on the control of forest termites
62 (Hua et al. 2015; Pietersen et al. 2015; Yang et al. 2007). In addition to their ecological value,
63 pangolins are extremely economically important animals. Pangolins are the most poached and
64 trafficked mammal in the world because of the high demand for their meat, which is a delicacy,
65 and their scales which are used in traditional medicine (Trageser et al. 2017).

66 *Manis javanica* is classified as critically endangered by The International Union for
67 Conservation of Nature (IUCN) Red List of Threatened Species, (2017; Prop), which has been
68 classified in an appendix I species by the Convention on International Trade in Endangered Species
69 of Wild Fauna and Flora (CITES I). The number of *M. javanica* in the wild is dramatically
70 declining for several reasons. A major threat is the rapid loss and deterioration of their natural
71 habitat, owing to deforestation activities; illegal hunting, which might reflect the pangolin's
72 economic value; and human agricultural expansion. Therefore, artificial breeding may be the best
73 choice for ensuring pangolin survival. A suitable artificial diet is one of the critical limiting factors
74 in raising pangolins in captivity. Pangolins have adapted to a highly specialized diet of ants and
75 termites, thus making it difficult to replace their natural food completely with artificial food (Hua
76 et al. 2015; Yang et al. 2007). Pangolins favor high-protein, high-fat, and high-calorie food, and
77 they have the notable ability to digest and absorb chitin in the digestive system (Hua et al. 2015;
78 Yang et al. 2007). Chitin is a linear polymer composed of N-acetyl-beta-glucosaminidase with a
79 beta-1, 4 glycosidic bond, which is one of substances contained in insect exoskeletons and the
80 peritrophic membranes of ants. Internal degradation of chitin particles is mainly performed by
81 chitinase (Strobel et al. 2013).

82 Over the past 150 years, several zoos have tried to maintain pangolins. However, because of
83 inadequate diets, these animals have not been successfully maintained for long periods by most
84 zoos (Hua et al. 2015). Some formulas for diets fed to *M. javanica* in captivity use a paste mixture
85 of several kinds of food such as egg (hard boiled), multivitamin liquid, horse meat, water,
86 mealworms, insectivore pellets, salmon oil, and powdered termite mound (Vijayan et al. 2009).

87 Digestive disorders often appear in pangolins fed with artificial food, and the feces of the animals
88 become fluid. Several researchers have suggested that a certain proportion of chitin might be the
89 key to artificial diets for pangolins (Ya-yong et al. 1999; Yang et al. 2007), but an understanding
90 of the molecular genetics is lacking, which might provide a theoretical basis for raising *M. javanica*
91 in captivity.

92 Genetic studies of endangered species have become increasingly widespread in the recent two
93 years (Choo et al. 2016; Mohamed Yusoff et al. 2016; Mwale et al. 2017; Zhihai et al. 2016).
94 Especially, the genomes and transcriptomes of *M. javanica* have been sequentially reported (Choo
95 et al. 2016; Mohamed Yusoff et al. 2016). Nowadays, more and more molecular information about
96 *M. javanica* can be available for the high-throughput next-generation sequencing (NGS)
97 technologies popping up like mushrooms. The complete genome sequencing of *M. javanica* and
98 transcriptome sequencing of eight organs, including the heart, liver, spleen, lung, kidney, thymus,
99 cerebellum, and cerebrum, have progressively revealed unknown aspects of pangolin biology. The
100 high-quality transcriptomes have been used for analyses of the functional and phylogenetic aspects
101 of immunity biology (Mohamed Yusoff et al. 2016), but genetic research regarding
102 myrmecophagy is still lacking. This observation led us to consider the molecular specificity of
103 pathways in myrmecophagy. What specific molecular pathways are involved in the evolution of
104 this dietary adaption, and how do they affect the appearance of this feature? In terms of dietary
105 adaptation, do specific genes exist for digestive function? Here, we selected liver, small intestine,
106 and salivary glands for transcriptome sequencing and analysis of the genetic selection or potential
107 candidate genes involved in myrmecophagy, which play an important role in the digestive system,

108 salivary glands is one of the important amylase secretory organs, there are a lot of amylase and
109 lipase contained in the secretions of liver, and the small intestine is involved in the absorption of
110 the nutriment, to analyze the unique feeding behavior of pangolins and to provide a new approach
111 to the protection of the pangolin.

112

113 **Materials and Methods**

114 **Ethics statement**

115 All animal procedures were approved by the ethics committee for animal experiments at the
116 Guangdong Institute of Applied Biological Resources (reference number: G2ABR20170523), and
117 followed basic principles.

118 **Biological sample**

119 Briefly, one female adult *M. javanica* sample were provided by the Dongguan Institute of
120 Qingfengyuan Animal Medicine (Dongguan, Guangdong, China). The specimen was dissected
121 immediately after their natural death. The salivary glands, liver, and small intestine were collected
122 as soon as possible, frozen in liquid nitrogen, and stored at -80°C until RNA extraction.

123 **RNA isolation, cDNA library construction and Illumina sequencing**

124 Total RNA of three tissues was extracted from tissues with RNAiso reagent (Takara, Otsu,
125 Japan) and was treated with DNase I (Takara). RNA purity was checked using the NanoPhotometer
126 spectrophotometer (IMPLEN, CA, USA). RNA concentration was measured using Qubit RNA
127 Assay Kit in Qubit 2.0 Fluorometer (Life Technologies, CA, USA). RNA integrity was assessed
128 using the RNA Nano 6000 Assay Kit of the Agilent Bioanalyzer 2100 system (Agilent

129 Technologies, CA, USA). RNA was frozen at -80°C until cDNA library construction.

130 RNA samples from three organs of sample 1 were sent for preprocessing, and the average
131 insert size was 200 bp. mRNA was purified from total RNA using poly-T oligo-attached magnetic
132 beads. DNA contaminants were further removed through DNase enzyme digestion followed by
133 rRNA removal. Then cDNA synthesis was performed, and was followed by PCR amplification to
134 generate a complete cDNA library, which was sent for sequencing using the Illumina HiSeq™
135 2000 platform.

136 **Data assembly and annotation**

137 Four groups of sequencing data were used for assembling and annotating, and one group was
138 selected from the sequenced liver from a published paper with National Center for Biotechnology
139 Information (NCBI) Sequence Read Archive (SRA) accession No.SRR2561213 (Mohamed
140 Yusoff et al. 2016). Primary sequencing data (raw reads) from the Illumina HiSeq™ 2000 were
141 subjected to quality control (QC) through in-house perl scripts to determine whether a
142 resequencing step was needed. Followed as: a) remove reads with adaptors, b) remove reads in
143 which unknown bases (N) are more than 5% (Parameters:-n 0.05), c) remove low quality reads
144 (we define the low quality read as the percentage of base which quality is lesser than 10 is greater
145 than 20% in a read) (Parameters:-l 10 -q 0.2). Clean reads were aligned to reference sequences
146 with a spliced read mapper for RNA-Seq-*TopHat2*
147 (<http://ccb.jhu.edu/software/tophat/index.shtml>), the reference sequences were the assembled
148 whole-genome sequences of *Malayan pangolin* which had been deposited at GenBank under the
149 accessions JSZB00000000.1. Then, the alignment data were used to calculate the distribution and

150 coverage of the reads on the reference genes.

151 Next, all the transcripts (>200 bp) were annotated on the basis of basic local alignment search
152 tool (BLASTX) results with e-values of $1e^{-5}$ against seven databases, including the non-redundant
153 protein database (NR, <ftp://ftp.ncbi.nih.gov/blast/db/>), a manually annotated, non-redundant
154 protein sequence database (Swiss-Prot, <http://www.uniprot.org/>), the Kyoto Encyclopedia of
155 Genes and Genomes (KEGG, <http://www.genome.jp/kegg/>), Cluster of Orthologous Groups
156 (COG, <http://www.ncbi.nlm.nih.gov/COG/>), Gene Ontology (GO,
157 <http://www.geneontology.org/>), the database of Clusters of Protein homology (KOG,
158 <http://www.ncbi.nlm.nih.gov/KOG/>) and the Translated EMBL Nucleotide Sequence Data Library
159 (TrEMBL, <http://www.bioinfo.pte.hu/more/TrEMBL.htm>) database. Furthermore, gene
160 expression analysis was performed, which included the gene expression level and differential gene
161 expression between every two groups of data.

162 **Correlation between any two pangolin tissue transcriptomes**

163 To examine the close relatedness of *M. javanica* organ transcriptomes, the expression levels
164 of the transcripts (FPKM) in the transcriptomes of each tissue were manipulated. By using the tool
165 “RSEM-calculate-expression” in the RSEM pipeline (<http://deweylab.biostat.wisc.edu/RSEM>),
166 which is an accurate transcript quantification software from RNA-Seq data with or without a
167 reference genome. The reads of each tissue were mapped to the transcripts (Li & Dewey 2011).
168 Gene expression values, expressed as $\log_{10}(\text{FPKM}+1)$ for the transcriptomic data from each
169 tissue were plotted against one another to produce scatter plots. R^2 values were then calculated
170 from the scatter plots to assess the correlation between any two *M. javanica* transcriptomes.

171

172 **Results**

173 **Illumina sequencing and assembly**

174 To obtain a comprehensive and representative transcriptome of *M. javanica*, 97,353,658 high-
175 quality clean reads (for a total length of 2,920,609,740 bp) were generated from the three tissues
176 after the removal of the adaptor sequences. All high-quality sequencing reads from *M. javanica*
177 are available on the NCBI Gene Expression Omnibus (GEO) database with the accession:
178 GSM2667949, GSM2667950 and GSM2667951. The average proportion of high-quality clean
179 reads was 95.58% (Table 1). The clean reads were assembled into long assembled sequences
180 (contigs) with *TopHat2*. The alignment efficiency between the sample and reference genome
181 ranged from 69.57% to 89.30% (Table 2). The ratio of the transcripts ranged from 76.11% to
182 85.16%, as compared with the exons (S1 Figure).

183 **Functional annotation**

184 From the *M. javanica* transcriptome, 22,538 transcripts (93.05%) were annotated on the basis
185 of the COG, GO, KEGG, KOG, Swiss-Prot, TrEMBL, and NR databases using BLAST. A total
186 of 6,228 transcripts were annotated against the COG database, followed by 13,977, 14,115, 16,648,
187 17,135, and 20,964 transcripts annotated on the basis of the KEGG, KOG, GO, Swiss-Prot, and
188 TrEMBL databases, respectively (S1 Table). As expected, the majority of the 22,473 transcripts
189 matched the NR databases (e-value $< 10^{-5}$) (S2 Figure and S1 File). The *M. javanica* transcripts
190 were annotated on the basis of the top BLASTX hits in the species distribution statistics. The top
191 five organisms were *Ceratotherium simum* (2,382 transcripts, 10.60%), *Equus caballus* (1,402,

192 6.24%), *Canis lupus* (1,349, 6.01%), *Mustela putorius* (1,044, 4.65%) and *Odobenus rosmarus*
193 (1,022, 4.55%) (S3 Figure).

194 **COG and KOG analysis**

195 In the COG database, the largest category of *M. javanica* annotated transcripts was general
196 function prediction only (R) (2,438 transcripts, 27.76%), which was followed by replication,
197 recombination, and repair (L) (848, 9.65%); transcription (K) (845, 9.62%); signal transduction
198 mechanisms (T) (790, 8.99%); and post-translational modification, protein turnover, and
199 chaperones (O) (484, 5.51%) (S4A Figure). In the KOG database, the largest category of *M.*
200 *javanica* annotated transcripts was general function prediction only (R) (2,910 transcripts, 18.3%),
201 followed by signal transduction mechanisms (T) (2,744, 17.26%); post-translational modification,
202 protein turnover, and chaperones (O) (1,259, 7.92%); function unknown (S) (1,182, 7.43%); and
203 transcription (K) (1070, 6.73%) (S4B Figure).

204 In both the COG and KOG analysis, several transcripts were involved in the transport and
205 metabolism of the three major nutrients: 136 transcripts were related to carbohydrate transport and
206 metabolism, 122 were related to lipid transport and metabolism, and 124 transcripts were related
207 to amino acid transport and metabolism, respectively (S2 File).

208 **Gene Ontology (GO)**

209 Annotation of the *M. javanica* transcripts with the GO database classified 16,649 transcripts
210 into 61 small classes in the three ontologies: biological process, molecular function, and cellular
211 component. A total of 44.36% of the transcripts were assigned to biological processes, 16.26% to
212 molecular functions, and 39.38% to cellular components.

213 In the biological process ontology, the most highly represented terms were cellular processes
214 (10,494, 63.03%), single-organism processes (9,554, 57.38%), and biological regulation (7,986,
215 47.97%). The fourth top represented term was metabolic process (7,173, 43.08%), which was
216 followed by response to stimulus (4,915, 29.52%), multicellular organismal process (3,644,
217 21.89%), signaling (3,161, 18.99%), localization (3,001, 18.03%), developmental process (2,890,
218 17.36%), and cellular component organization or biogenesis (2,667, 16.02%). The terms
219 associated with biological regulation and metabolic process might be indicative of the involvement
220 of the *M. javanica* transcriptome in various digestive activities.

221 For molecular functions, the sequences were mainly assigned to binding (9,371, 56.29%) and
222 catalytic activity (5347, 32.12%). These were followed by molecular transducer activity (1,750,
223 10.51%), receptor activity (1,681, 10.1%) and transporter activity (1,026, 6.16%), which might be
224 involved in food digestion and absorption.

225 As anticipated, cell part (11,445, 68.74%) and cell (11,412, 68.54%) were the predominant
226 terms assigned to the pangolin transcriptome in cellular components and were followed by
227 organelle (8,014, 48.14%), membrane (5,980, 35.92%), membrane part (4,441, 26.67%), organelle
228 part (4,079, 24.5%), macromolecular complex (3,413, 20.5%) and extracellular region (1,044,
229 6.27%) (S5 Figure and S3 File). Overall, these results indicate the broad range of biological
230 activities related to the expressed pangolin transcriptome, representing a pooled collection of the
231 three digestive tissues sequenced.

232 **KEGG pathway analysis**

233 To identify the pathways in which the transcripts of *M. javanica* were involved, the transcripts

234 were mapped on the basis of KEGG pathways. A total of 13,977 (57.71%) *M. javanica* transcripts
235 were associated with 290 unique KEGG pathways, with a total of 15 representing cellular
236 processes, followed by 22, 27, 66, 68, and 89 unique KEGG pathways representing genetic
237 information passing, environmental information processing, organismal systems, human diseases,
238 and metabolism, respectively (S4 File).

239 The most-represented pathways in the *M. javanica* transcripts included olfactory transduction
240 (969 transcripts) and pathways in cancer (444 transcripts), followed by the PI3K-Akt signaling
241 pathway (391 transcripts), MAPK signaling pathway (300 transcripts), and neuroactive ligand-
242 receptor interaction (292 transcripts) (S6 Figure). The sense of smell is closely related to the
243 biological activity of instinctive behavior such as feeding. The olfactory pathway plays a key role
244 in the specific recognition ability of smell, thus leading the animal to different foods. A total of
245 969 genes were associated with olfactory transduction in *M. javanica* transcripts, 942 transcripts
246 of which were annotated as various kinds of olfactory receptors. These finding might lead to a
247 keen sense of smell in *M. javanica*.

248 **Metabolic pathway analysis**

249 A total of 1,814 transcripts were associated with 89 unique metabolic pathways of KEGG.
250 Most transcripts were enriched in lipid metabolism (431 transcripts), carbohydrate metabolism
251 (365 transcripts), amino acid metabolism (321 transcripts), glycan biosynthesis and metabolism
252 (271 transcripts), nucleotide metabolism (233 transcripts), and metabolism of cofactors and
253 vitamins (225 transcripts). Other transcripts were associated with global and overview maps (199
254 transcripts), energy metabolism (167 transcripts), metabolism of other amino acids (119

255 transcripts), and xenobiotics biodegradation and metabolism (116 transcripts), and the smallest
256 number of the transcripts were associated with terpenoid and polyketide metabolism (27
257 transcripts) and secondary metabolite biosynthesis (13 transcripts) (Fig 1A).

258 **Carbohydrate metabolism**

259 Inositol phosphate metabolism (73 transcripts), glycolysis/gluconeogenesis (70 transcripts),
260 starch and sucrose metabolism (57 transcripts), and amino sugar and nucleotide sugar metabolism
261 (53 transcripts) were at the top of the carbohydrate metabolic lists, whereas ascorbate and aldarate
262 metabolism were at the bottom.

263 The chitin-degrading enzyme acidic mammalian chitinase (CHIA), which is involved in the
264 degradation of the chitin in the insect cuticle and the peritrophic membrane of the ant diet, was
265 found in the amino sugar and nucleotide sugar metabolism pathway (KEGG: 00520), thus
266 suggesting that this pathway may be directly involved in ant digestion by *M. javanica* (Fig 1B).

267 **Lipid metabolism**

268 Glycerophospholipid metabolism (100 transcripts), arachidonic acid metabolism (76
269 transcripts), steroid hormone biosynthesis (68 transcripts), and sphingolipid metabolism (55
270 transcripts) were at the top of the lipid metabolic list; in contrast, fatty acid biosynthesis (55
271 transcripts) was at the bottom. We identified transcripts from several pathways in unsaturated fatty
272 acid metabolism, including arachidonic acid metabolism (76 transcripts), linoleic acid metabolism
273 (36 transcripts), alpha-linolenic acid metabolism pathways (23 transcripts), and biosynthesis of
274 unsaturated fatty acids (23 transcripts) (Fig 1C).

275 **Amino acid metabolism**

276 Lysine degradation (66 transcripts), valine, leucine and isoleucine degradation (65
277 transcripts), arginine and proline metabolism (64 transcripts), and tryptophan metabolism (35
278 transcripts) were at the top of the amino acid metabolic lists. The biosynthesis pathways of some
279 amino acids, such as phenylalanine, tyrosine, and tryptophan biosynthesis (6 transcripts); valine,
280 leucine and isoleucine biosynthesis (5 transcripts); and lysine (2 transcripts) were at the bottom
281 (Fig 1D). None of the transcripts were found to be involved in arginine biosynthesis.

282 **Metabolism of cofactors and vitamins, and terpenoids and polyketides**

283 Retinol metabolism (65 transcripts), porphyrin and chlorophyll metabolism (46 transcripts),
284 nicotinate and nicotinamide metabolism (36 transcripts), and pantothenate and CoA biosynthesis
285 (31 transcripts) were at the top of the metabolism of cofactors and vitamins lists. There was only
286 one list in the terpenoids and polyketides, which was terpenoid backbone biosynthesis (27
287 transcripts) (Fig 1E), as shown in Fig 2.

288 **Annotation of the new transcripts**

289 On the basis of the genome sequences of *M. javanica*, Cufflinks software was used for joining
290 the mapped reads together, comparing them with the annotated information for the original
291 genome, and searching for the gapped sequences, which were not annotated. A total of 3,373 new
292 transcripts were discovered in the results (S5 File), from which 1,459 transcripts were annotated
293 on the basis of the COG, GO, KEGG, KOG, Swiss-Prot, TrEMBL and NR databases by using
294 BLAST (S2 Table and S6 File).

295 In Gene Ontology analysis, 75 new transcripts were involved in 22 metabolic categories.
296 Some of the new genes were involved in the inositol metabolic process (GO: 0006020), for

297 example, *Manis_javanica_newGene_958*, and some were involved in the linoleic acid metabolic
298 process (GO: 0043651), for example, *Manis_javanica_newGene_12722*. For KEGG, 114 new
299 genes were related to metabolic function, including lipid metabolism (41 transcripts), carbohydrate
300 metabolism (24 transcripts), cofactor and vitamin metabolism (22 transcripts), and amino acid
301 metabolism (20 transcripts) (S7 Figure).

302 **Gene expression repertoire**

303 Distributions of potential transcripts related to feeding among the three tissue libraries are
304 shown in Table 3, S3 Table and S7 File, including the 997 transcripts related to sensory perception.
305 972 of these transcripts were related to olfaction, and 11 and 14 transcripts were related to vision
306 and taste, respectively. A total of 133 transcripts were related to digestive enzyme gene families,
307 and 70 of these transcripts were related to lipid degradation, and 39 and 20 transcripts were related
308 to the degradation of proteins and carbohydrates, respectively. These genes were considered to be
309 involved in the profile of food choice, digestion and absorption, which might serve as a molecular
310 mechanism in myrmecophagy. Among these transcripts, acidic mammalian chitinase (*CHIA*),
311 chitinase-3-like protein 1 (*CHI3L1*), and chitinase domain-containing protein 1 (*CHID1*) were
312 related to chitin degradation. A total of 199 transcripts were related to molecular transporters,
313 including sugar transporters, aa transporters, apolipoprotein transporters, cationic/anion
314 transporters, vitamin transporters, cotransporters and others, among which, the UDP-N-
315 acetylglucosamine transporter (*SLC35A3*, *SLC35B4*, and *SLC35D2*) was related to the decomposer
316 absorption of the chitin unit which was N-acetylglucosamine.

317 **Pairwise comparisons of different transcriptomic profiles**

318 To examine the similarity among organ transcriptomes, we performed statistical correlation
319 analysis for each pair of organs by using $\log_{10}(\text{FPKM}+1)$ to normalize the plots (Fig 3). Our data
320 showed that the two liver transcriptomes had the most similar expression profiles (coefficient of
321 determination, $R^2=0.53$), followed by the liver and gut ($R^2=0.30$). The salivary glands and gut had
322 the least similar transcriptomic profiles with $R^2=2e^{-0.4}$. The results reflected the varying complexity
323 between the same organs in different individuals, possibly because one of the two specimens was
324 pregnant. The differences between every two organs compared reflected the different digestive
325 functions of the three organs.

326 A total of 11,055 transcripts were expressed ($\text{FPKM}>1.0$) in all three tissues, of which 3,947
327 transcripts were annotated in KEGG. Several transcripts were enriched in lipid metabolism (214
328 transcripts), carbohydrate metabolism (240 transcripts), and amino acid metabolism (188
329 transcripts) (Fig 4). Other transcripts near the top of the metabolic lists included
330 glycerophospholipid metabolism (62 transcripts); valine, leucine and isoleucine degradation (53
331 transcripts); lysine degradation (49 transcripts); and inositol phosphate metabolism (45
332 transcripts). The biosynthesis pathways of valine, leucine, and isoleucine biosynthesis (1
333 transcripts) and lysine (2 transcripts) were less commonly represented.

334 Differentially expressed genes were identified among systems in the metabolic pathways of
335 sugars, lipids, and amino acids. A total of 382 transcripts were differentially expressed between
336 the small intestine and liver, compared with 258 transcripts differentially expressed between the
337 salivary glands and small intestine. The numbers of the different genes were 23 and 27 in the starch

338 and sucrose metabolism and arginine and proline metabolism between the small intestine and liver,
339 respectively, whereas 31 genes were in the steroid hormone biosynthesis between the liver and the
340 referred liver (S8 Figure).

341 Several transcripts were specifically expressed in the single sample, including 21 transcripts
342 in the small intestine that were involved in 19 pathways, five transcripts in the liver that were
343 involved in 11 pathways, 36 transcripts in the referred liver that were involved in 27 pathways,
344 and six transcripts in the salivary glands that were involved in 10 pathways (S4 Table). The highest
345 number of specific transcripts was eight, and these transcripts were involved in the arachidonic acid
346 metabolism of the transcriptional results of the liver from the previous study; six transcripts were
347 involved in glycerophospholipid metabolism, in either lipid metabolism or arachidonic acid
348 metabolism of the small intestine (Fig 5).

349

350 Discussion

351 Malaysian pangolins are unique endangered mammals. Captive breeding of this species
352 provides an opportunity to study the molecular mechanisms of myrmecophagy. Here,
353 transcriptome sequencing of digestive organs was performed to observe the metabolic pathways
354 and functional genes related to the myrmecophagy in an attempt to understand the molecular
355 mechanisms involved in myrmecophagy. The results may provide an important theoretical basis
356 for the successful captive breeding of the species. The transcriptomic data of the three organs
357 showed a high degree of confidence, and the transcripts were well annotated, thus providing a
358 genomic and molecular basis for future study of this lesser-known unique mammalian species.

359 Functional annotation of the *M. javanica* transcripts revealed the involvement of molecular
360 mechanisms in various essential KEGG pathways, such as the olfactory transduction, amino sugar
361 and nucleotide sugar metabolism, lipid metabolism and terpenoid and polyketide metabolism
362 pathways, which may support the myrmecophagous feeding habits of this mammalian species,
363 including diet selection, digestion and absorption.

364 Ants are a high-lipid, high-protein food (Tomotake et al. 2010). They contain more than 50%
365 crude protein, as determined according to a nutritional value evaluation, and contain more than 20
366 kinds of amino acids; varied microelements; special chemicals, such as formic acid and
367 herbaceous acetaldehyde, which are all triterpenoid compounds; and multivitamins
368 (Pattarayingsakul et al. 2017). Many pangolin genes are likely to be involved in the digestion of
369 these materials, because there were 27 transcripts related to the biosynthesis of terpenoid
370 backbone, which might be one of biological basis for their adaptations to ant-eating habits found in
371 our transcriptomic results. However, no genes were found to participate in the pathway of
372 arginine synthesis, according to the KEGG analysis, and only two transcripts were involved in the
373 synthesis of lysine. Few transcripts were involved in the synthesis pathways of the essential amino
374 acids in humans, such as, lysine, valine, leucine, isoleucine, phenylalanine, and tryptophan (Galili
375 et al. 2016; Zhenyukh et al. 2017). These results suggested that *M. javanica* may synthesize
376 arginine de novo. Therefore, both essential amino acids and arginine must be added to
377 manufactured feed.

378 Chitin, one of the main components of the epidermis of ants and termites, is made of N-acetyl-
379 D-glucosamines (GluNAc) connected by a β -1, 4 glycosidic bond. Chitin can be digested only

380 with chitinase and acidic mammalian chitinase (*AMCase*); *AMCase* is widely found in the
381 digestive organs of animals (Eurich et al. 2009; Krykbaev et al. 2010; Pietersen et al. 2015; Strobel
382 et al. 2013). The origination of the digestive processes might be closely related to the activity of
383 *AMCase*, which determines the start of the chitin decomposition. The transporter genes of UDP-
384 N-acetyl glucosamine (*SLC35A3*, *SLC35B4*, and *SLC35D2*) might be directly related to the
385 absorption of the carbohydrate units during the process of chitin digestion. Therefore, chitin should
386 be added to the formulated diets to aid in digestion and absorption of nutrients. This suggestion is
387 consistent with the referenced formulas mentioned in Vijayan *et al* (Vijayan et al. 2009).

388 A total of 3,373 new genes were discovered in the transcriptomic datasets, of which 1459
389 were annotated, and 75 new genes were involved in metabolism. The new genes provided new
390 information for studying the myrmecophagous mechanisms of pangolins. A large number of genes
391 were expressed in all three tissues, whereas several specific genes in the three systems played
392 different roles in the metabolism of sugars, lipids, and amino acids, and the digestive functions of
393 the small intestine and salivary gland were relatively similar, in contrast to the differences between
394 the small intestine and liver. The functions of the livers from the two different individuals were
395 relatively different in the pathways of lipid metabolism, thus suggesting that the ratio of lipid in
396 the feed should be changed appropriately during pregnancy.

397 Overall, the smell of the formulated diet may be important for *M. javanica* with a strong sense
398 of smell. Diets with high-fat and high-protein content are conducive to pangolin management. In
399 addition, lysine, arginine and chitin could be added to the formulas to aid in the digestion and
400 absorption of the nutrients. Some indications suggested that changes in the fat content might be

401 appropriate during pregnancy.

402 In conclusion, *M. javanica* transcriptomic datasets of the three representative tissues would
403 provide the first-hand knowledge for uncovering the mysteries of the genetic mechanisms of
404 digestion and reproduction in this rare and unique mammal. For further, more and more
405 organizations involved in digestion, such as tongue, stomach, and pancreas, would be collected for
406 studying myrmecophagy. All these results would be gathered to unveil the mysteries of the special
407 diet of *M. javanica*.

408

409 **Acknowledgments**

410 We acknowledge BMKCloud (Beijing, China) for the data analysis. We acknowledge the
411 Dongguan Institute of Qingfengyuan Animal Medicinal (Dongguan, Guangdong, China) for their
412 selfless offering of three female pangolin samples.

413 Funding Sources: This project was supported by the Planning Funds of Scientific and
414 Technological of Guangdong Province (2016B070701016) and the Training Fund of Guangdong
415 Institute of Applied Biological Resources for Postdoctoral Researchers (NO.GIABR-pyjj201601),
416 the Funds for Environment Construction and Capacity Building of GDAS' Research Platform (xm-
417 2015081), GDAS Special Project of Science and Technology Development (2017GDASCX-
418 0107).

419

420 **References**

421 2017. The IUCN Red List of Threatened Species. Version 2017-1. www.iucnredlist.org.
422 Choo SW, Rayko M, Tan TK, Hari R, Komissarov A, Wee WY, Yurchenko AA, Kliver S, Tamazian G, Antunes A, Wilson

- 423 RK, Warren WC, Koepfli K-P, Minx P, Krasheninnikova K, Kotze A, Dalton DL, Vermaak E, Paterson IC,
424 Dobrynin P, Sitam FT, Rovie-Ryan JJ, Johnson WE, Yusoff AM, Luo S-J, Karuppanan KV, Fang G, Zheng D,
425 Gerstein MB, Lipovich L, O'Brien SJ, and Wong GJ. 2016. Pangolin genomes and the evolution of
426 mammalian scales and immunity. *Genome Research* 26:1312-1322.
- 427 Eurich K, Segawa M, Toei-Shimizu S, and Mizoguchi E. 2009. Potential role of chitinase 3-like-1 in inflammation-
428 associated carcinogenic changes of epithelial cells. *World J Gastroenterol* 15:5249-5259.
- 429 Galili G, Amir R, and Fernie AR. 2016. The Regulation of Essential Amino Acid Synthesis and Accumulation in Plants.
430 *Annual Review of Plant Biology* 67:153-178.
- 431 Hua L, Gong S, Wang F, Li W, Ge Y, Li X, and Hou F. 2015. Captive breeding of pangolins: current status, problems
432 and future prospects. *ZooKeys* 507:99-114.
- 433 Krykbaev R, Fitz LJ, Reddy PS, Winkler A, Xuan D, Yang X, Fleming M, and Wolf SF. 2010. Evolutionary and
434 biochemical differences between human and monkey acidic mammalian chitinases. *Gene* 452:63-71.
- 435 Li B, and Dewey CN. 2011. RSEM: accurate transcript quantification from RNA-Seq data with or without a reference
436 genome. *BMC Bioinformatics* 12:323.
- 437 Meyer W, Liamsiricharoen M, Suprasert A, Fleischer LG, and Hewicker-Trautwein M. 2013. Immunohistochemical
438 demonstration of keratins in the epidermal layers of the Malayan pangolin (*Manis javanica*), with remarks
439 on the evolution of the integumental scale armour. *Eur J Histochem* 57:e27.
- 440 Mohamed Yusoff A, Tan TK, Hari R, Koepfli K-P, Wee WY, Antunes A, Sitam FT, Rovie-Ryan JJ, Karuppanan KV,
441 Wong GJ, Lipovich L, Warren WC, O'Brien SJ, and Choo SW. 2016. De novo sequencing, assembly and
442 analysis of eight different transcriptomes from the Malayan pangolin. *Scientific Reports* 6:28199.
- 443 Mwale M, Dalton DL, Jansen R, De Bruyn M, Pietersen D, Mokgokong PS, and Kotze A. 2017. Forensic application of
444 DNA barcoding for identification of illegally traded African pangolin scales. *Genome* 60:272-284.
- 445 Pattarayingsakul W, Nilavongse A, Reamtong O, Chittavanich P, Mungsantisuk I, Mathong Y, Prasitwuttisak W, and
446 Panbangred W. 2017. Angiotensin-converting enzyme inhibitory and antioxidant peptides from digestion
447 of larvae and pupae of Asian weaver ant, *Oecophylla smaragdina*, Fabricius. *Journal of the Science of Food*
448 *and Agriculture* 97:3133-3140.
- 449 Pietersen DW, Symes CT, Woodborne S, McKechnie AE, and Jansen R. 2015. Diet and prey selectivity of the
450 specialist myrmecophage, Temminck's ground pangolin. *Journal of Zoology*.
- 451 Prop CC. 13. 2000. Transfer of *Manis crassicaudata*, *M. pentadactyla*, *M. javanica* from Appendix II to Appendix I.
452 India, Nepal, Sri Lanka and the United States of America.
- 453 Strobel S, Roswag A, Becker NI, Trenczek TE, and Encarna O JA. 2013. Insectivorous Bats Digest Chitin in the
454 Stomach Using Acidic Mammalian Chitinase. *PLoS ONE* 8:e72770.
- 455 Tomotake H, Katagiri M, and Yamato M. 2010. Silkworm pupae (*Bombyx mori*) are new sources of high quality
456 protein and lipid. *J Nutr Sci Vitaminol (Tokyo)* 56:446-448.
- 457 Trageser SJ, Ghose A, Faisal M, Mro P, Mro P, and Rahman SC. 2017. Pangolin distribution and conservation status
458 in Bangladesh. *PLoS ONE* 12:e0175450.
- 459 Vijayan M, Yeong C, and Ling D. 2009. Captive management of Malayan pangolins *Manis javanica* in the Night
460 Safari. WORKSHOP ON TRADE AND CONSERVATION OF PANGOLINS NATIVE TO SOUTH AND SOUTHEAST
461 ASIA. p 119.
- 462 Ya-yong K, Hong C, Shi-bao W, Qian L, and Gan-xin F. 1999. A study on Chinese pangolin's main food nutrition.
463 *Zoological Research* 20:394-395.

- 464 Yang CW, Chen S, Chang CY, Lin MF, Block E, Lorentsen R, Chin JS, and Dierenfeld ES. 2007. History and dietary
465 husbandry of pangolins in captivity. *Zoo Biol* 26:223-230.
- 466 Zhenyukh O, Civantos E, Ruiz-Ortega M, Sánchez MS, Vázquez C, Peiró C, Egado J, and Mas S. 2017. High
467 concentration of branched-chain amino acids promotes oxidative stress, inflammation and migration of
468 human peripheral blood mononuclear cells via mTORC1 activation. *Free Radical Biology and Medicine*
469 104:165-177.
- 470 Zhihai H, Jiang X, Shuiming X, Baosheng L, Yuan G, Chaochao Z, Xiaohui Q, Wen X, and Shilin C. 2016. Comparative
471 optical genome analysis of two pangolin species: *Manis pentadactyla* and *Manis javanica*. *Gigascience* 5:1-
472 5.
- 473

Figure 1

The metabolic pathway analysis of transcripts from *M. javanica*.

The x-axis shows the numbers of annotated transcripts in one class, and the y-axis shows the KEGG function classes.

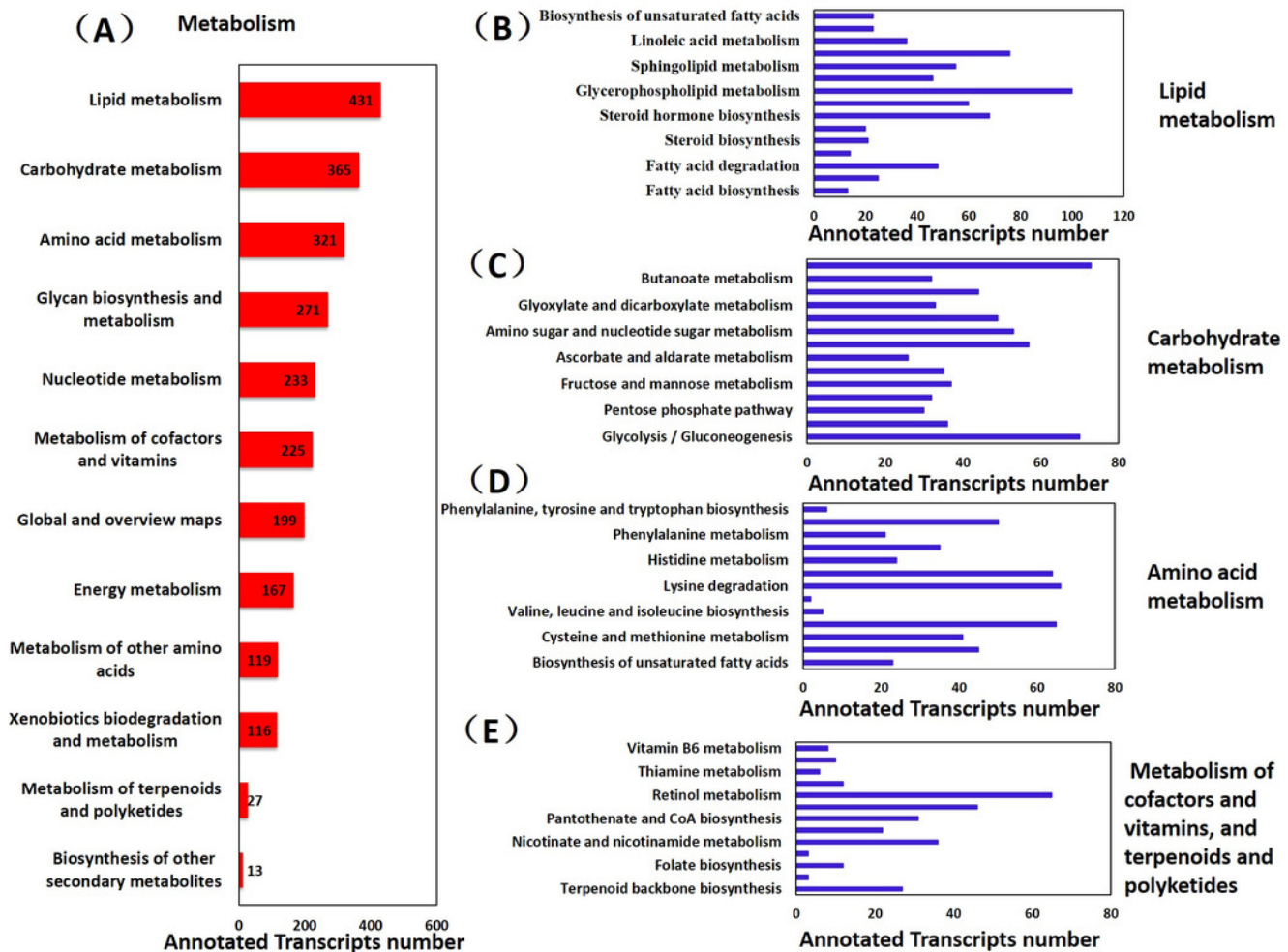


Figure 2

Terpenoid backbone biosynthesis (KEGG map 00900).

TERPENOID BACKBONE BIOSYNTHESIS

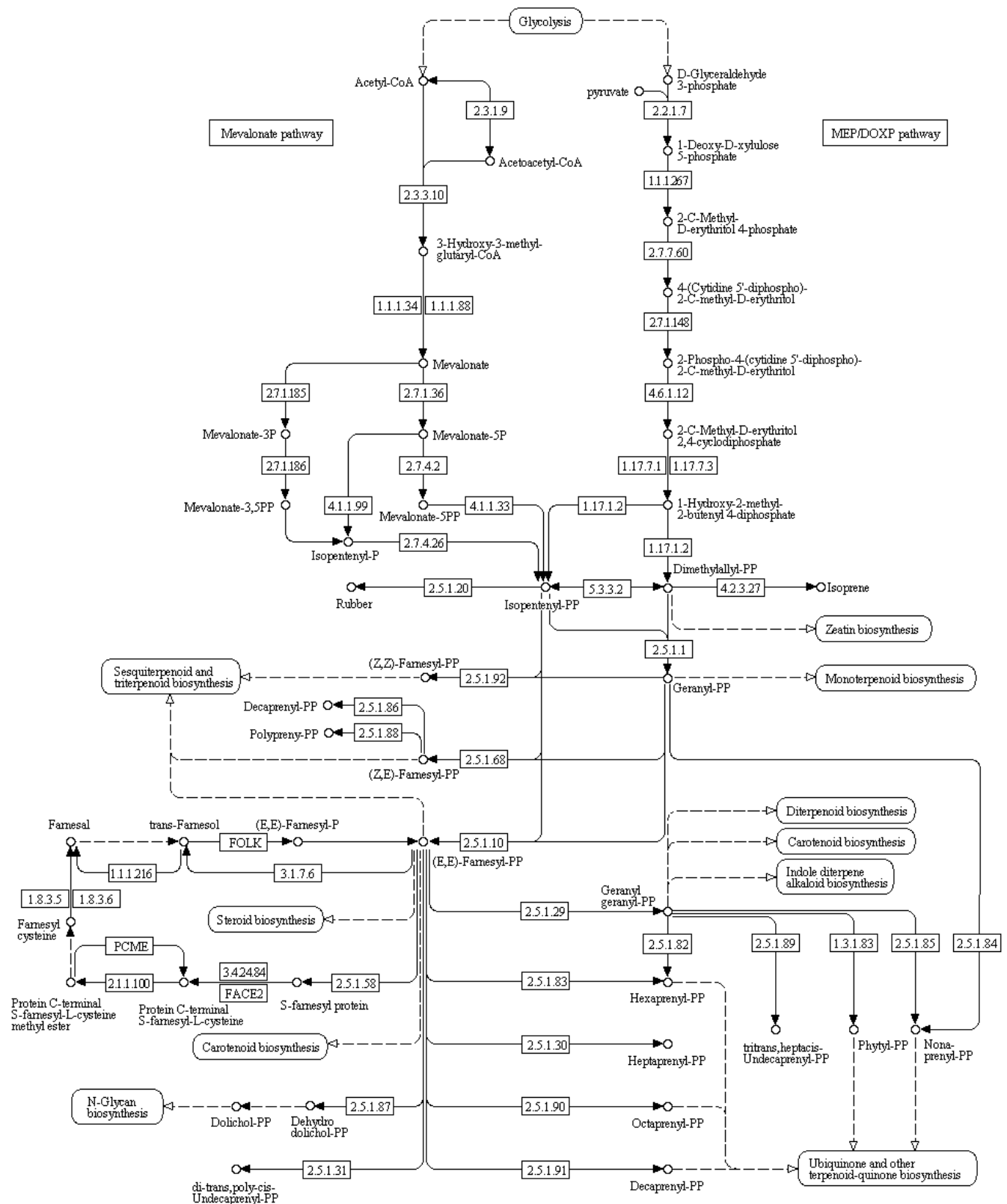


Figure 3

Correlation between any two organs.

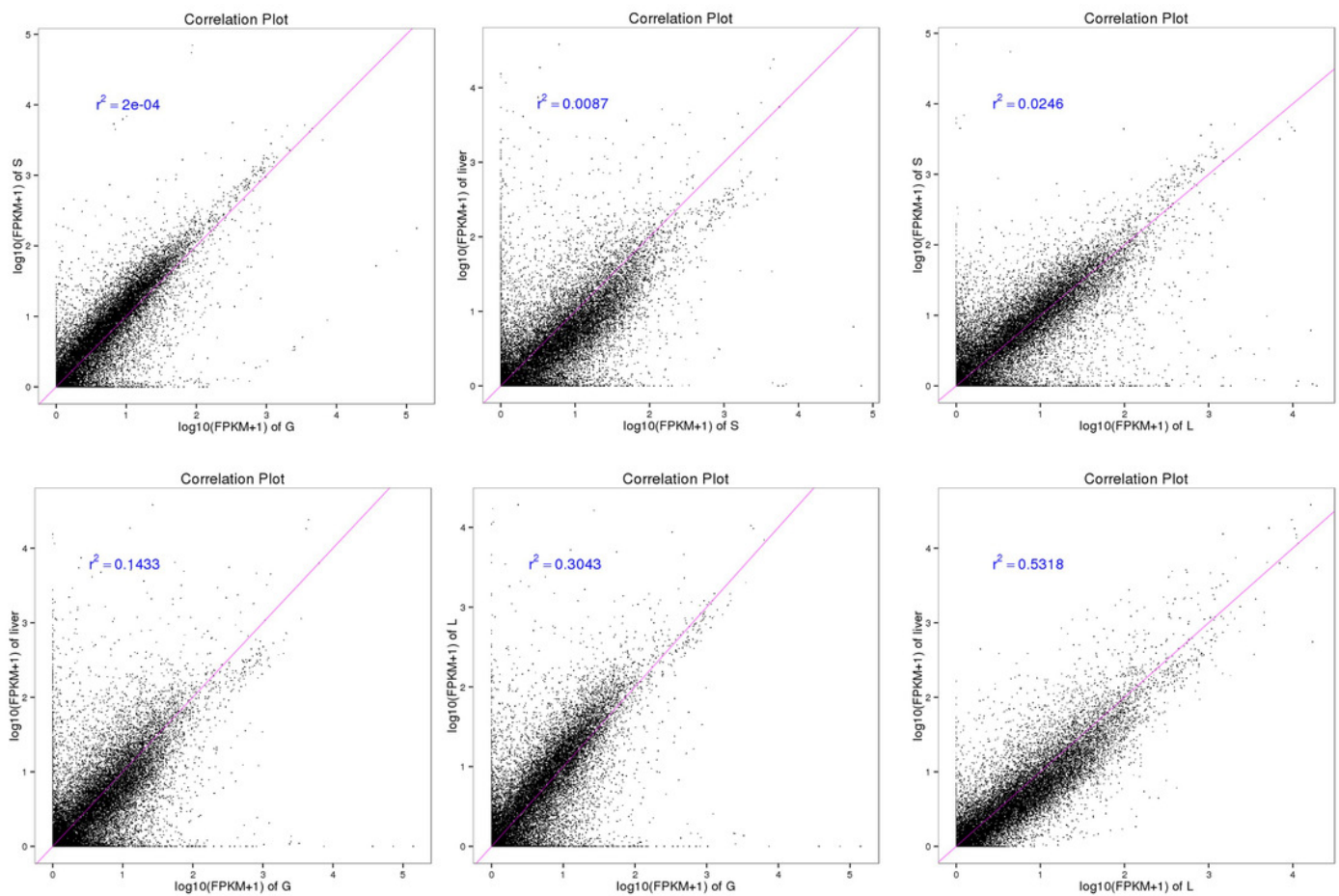


Figure 4

The transcripts related to metabolic pathways expressed in all three tissues.

The x-axis shows the number of transcripts with the KEGG function class, which was shown above the column, and the y-axis shows the KEGG function classes.

The transcripts related to metabolic pathways expressed in all three tissues

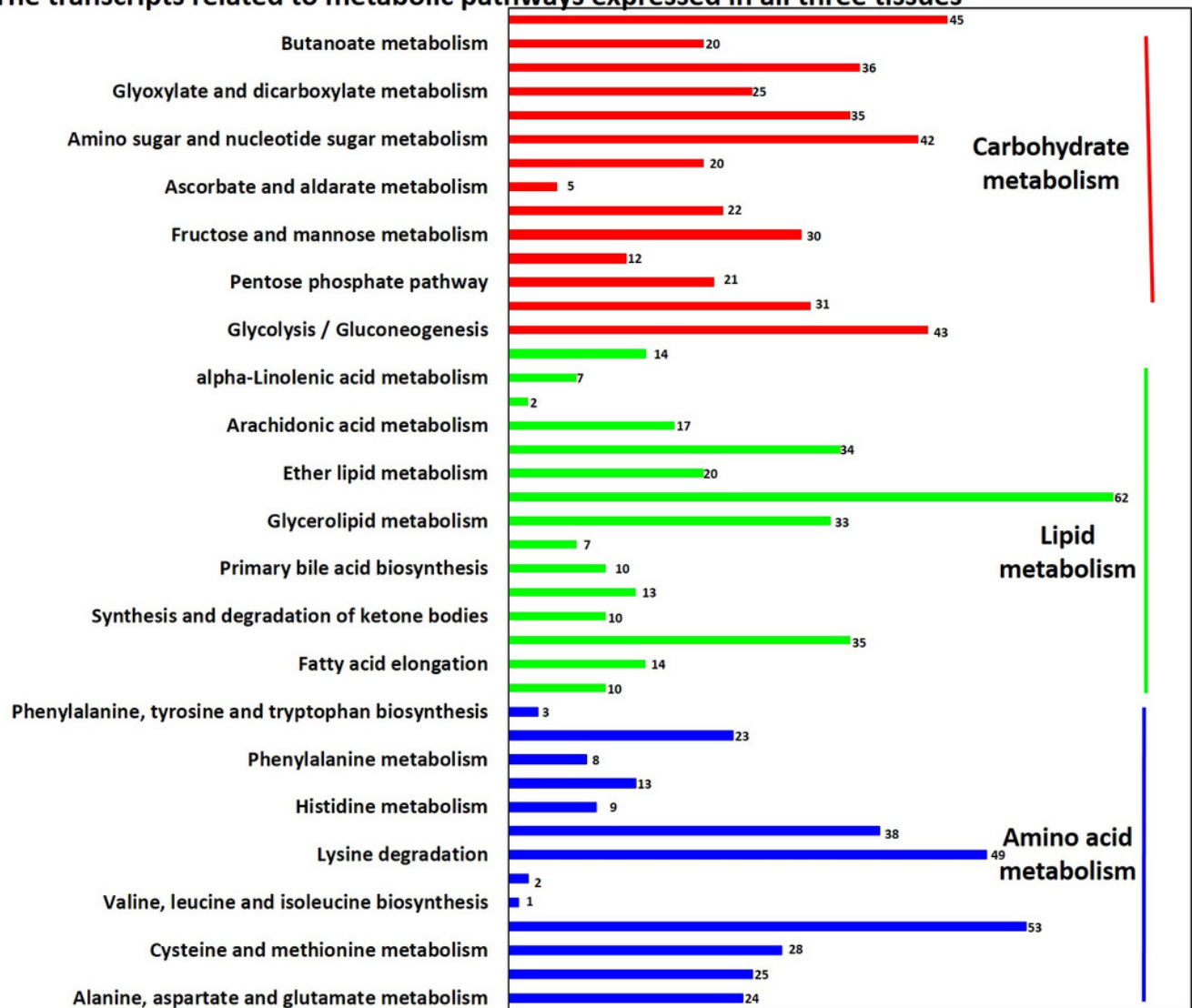


Figure 5

The number of transcripts related to metabolic pathways specifically expressed in the three tissues.

The x-axis shows the KEGG function classes, and the y-axis shows the number of transcripts with the corresponding KEGG function class.

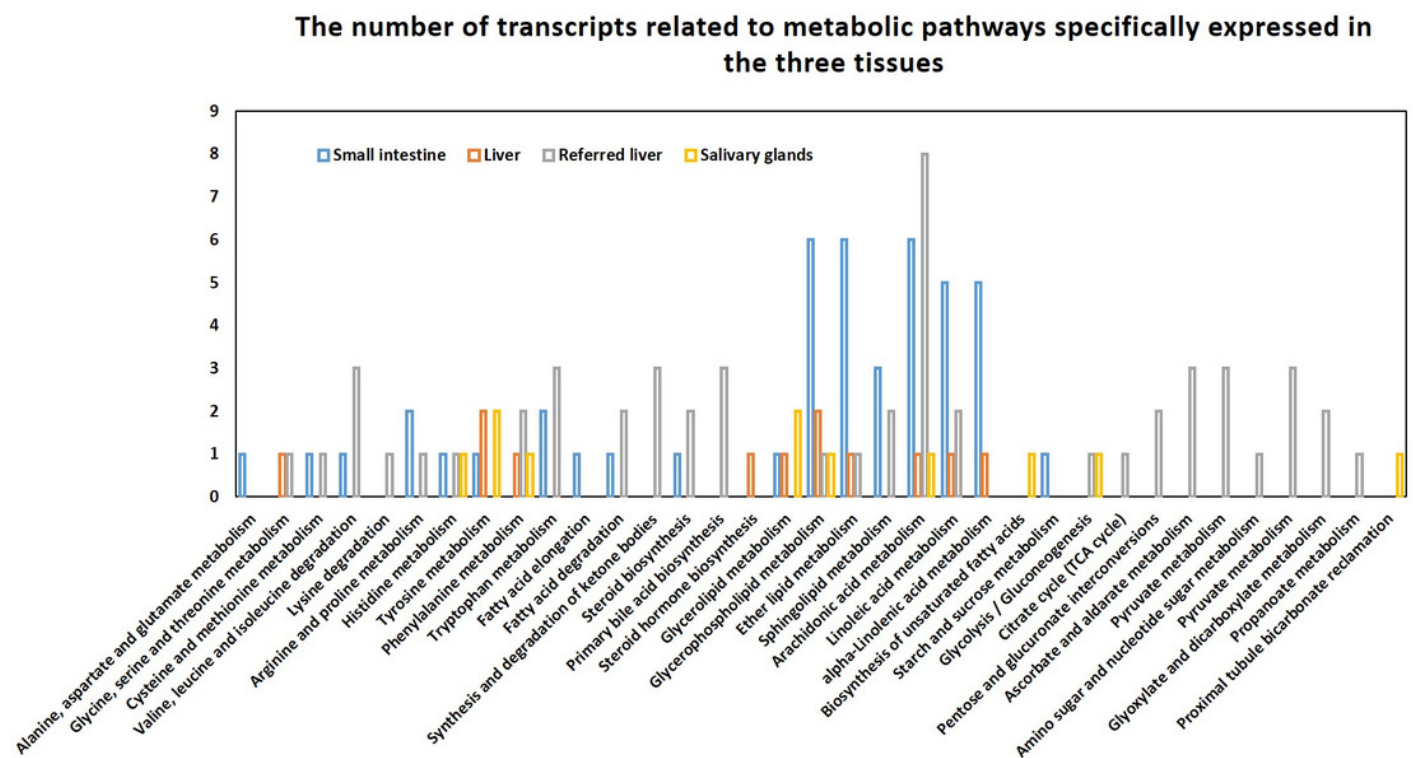


Table 1 (on next page)

output statistics of sequencing.

1
2

ID	Raw pairs (bp)	Clean pairs (bp)	Clean bases (bp)	GC Content	%\geqQ30%
Small intestine	20,296,915	15,117,014	4,535,104,200	53.71%	95.30%
Liver	33,288,751	22,073,184	6,621,955,200	53.15%	94.67%
Salivary glands	20,297,074	14,857,037	4,457,111,100	51.33%	95.58%
Referred liver	-	45,306,423	9,061,284,600	50.87%	90.35%

Table 2 (on next page)

The results of sequencing data aligned to the *Manis.javanica* genome.

ID	Total Reads	Mapped Reads	Uniq Mapped Reads	Multiple Map Reads
Small intestine	30,234,028	22,277,733 (73.68%)	21,843,354 (72.25%)	434,379 (1.44%)
Liver	44,146,368	31,965,251 (72.41%)	31,694,559 (71.79%)	270,692 (0.61%)
Salivary glands	29,714,074	20,673,075 (69.57%)	19,911,660 (67.01%)	761,415 (2.56%)
Referred liver	90,612,846	80,913,231 (89.30%)	80,064,920 (88.36%)	848,311 (0.94%)

Table 3 (on next page)

Genes related to the diet of *M.javanica*.

Type	Gene name
Opsin	GRK1, OPN1SW, OPN1LW, OPN4, PDE6D, PDE6G, PDE6H, RHO
Taste	TAS1R2, TAS1R3, TAS2R1, TAS2R4, TAS2R7, TAS2R10, TAS2R30, TAS2R38, TAS2R40
Olfactory	CNGA2, DTMT, OLF1, OLF2, OLF3, OLF4, OR1A1, OR1D2, OR1E1, OR1E2, OR1E5, OR1G1, OR3A1, OR3A2, OR3A3
Carbohydrases	AGL, AMY2, CHIA, CHI3L1, CHID1, GAA, GANAB, GANC, GBA3, GLB1, GLB1L, PRKCSH, SI
Lipases	ABHD6, ABHD12, CEL, CLPS, DDHD1, GPLD1, Group XV phospholipase A2, LIPA, LIPC, LIPE, LIPF, LIPH, LMF1, LMF2, LPL, LYPLAL1, NAPEPLD, PLA1A, PLA2G1B, PLA2G2A, PLA2G3, PLA2G4A, PLA2R1, PLB1, PLBD1, PLBD2, PLD3, PNLIP, PNLIPRP1, PNLIPRP2, PNPLA2, PNPLA8
Protease	Anionic trypsin, ANPEP, Cationic trypsin, CELA1, Chymotrypsin A chain C, CTB1, CTB2, CTB3, CTB4, CTB5, CTB6, CTB7, CTB8, CTB9, CTB10, CTB11, CTB12, CTB13, CTB14, CTB15, CTB16, CTB17, CTB18, CTB19, CTB20, CTB21, CTB22, CTB23, CTB24, CTB25, CTB26, CTB27, CTB28, CTB29, CTB30, CTB31, CTB32, CTB33, CTB34, CTB35, CTB36, CTB37, CTB38, CTB39, CTB40, CTB41, CTB42, CTB43, CTB44, CTB45, CTB46, CTB47, CTB48, CTB49, CTB50, CTB51, CTB52, CTB53, CTB54, CTB55, CTB56, CTB57, CTB58, CTB59, CTB60, CTB61, CTB62, CTB63, CTB64, CTB65, CTB66, CTB67, CTB68, CTB69, CTB70, CTB71, CTB72, CTB73, CTB74, CTB75, CTB76, CTB77, CTB78, CTB79, CTB80, CTB81, CTB82, CTB83, CTB84, CTB85, CTB86, CTB87, CTB88, CTB89, CTB90, CTB91, CTB92, CTB93, CTB94, CTB95, CTB96, CTB97, CTB98, CTB99, CTB100, CTB101, CTB102, CTB103, CTB104, CTB105, CTB106, CTB107, CTB108, CTB109, CTB110, CTB111, CTB112, CTB113, CTB114, CTB115, CTB116, CTB117, CTB118, CTB119, CTB120, CTB121, CTB122, CTB123, CTB124, CTB125, CTB126, CTB127, CTB128, CTB129, CTB130, CTB131, CTB132, CTB133, CTB134, CTB135, CTB136, CTB137, CTB138, CTB139, CTB140, CTB141, CTB142, CTB143, CTB144, CTB145, CTB146, CTB147, CTB148, CTB149, CTB150, CTB151, CTB152, CTB153, CTB154, CTB155, CTB156, CTB157, CTB158, CTB159, CTB160, CTB161, CTB162, CTB163, CTB164, CTB165, CTB166, CTB167, CTB168, CTB169, CTB170, CTB171, CTB172, CTB173, CTB174, CTB175, CTB176, CTB177, CTB178, CTB179, CTB180, CTB181, CTB182, CTB183, CTB184, CTB185, CTB186, CTB187, CTB188, CTB189, CTB190, CTB191, CTB192, CTB193, CTB194, CTB195, CTB196, CTB197, CTB198, CTB199, CTB200, CTB201, CTB202, CTB203, CTB204, CTB205, CTB206, CTB207, CTB208, CTB209, CTB210, CTB211, CTB212, CTB213, CTB214, CTB215, CTB216, CTB217, CTB218, CTB219, CTB220, CTB221, CTB222, CTB223, CTB224, CTB225, CTB226, CTB227, CTB228, CTB229, CTB230, CTB231, CTB232, CTB233, CTB234, CTB235, CTB236, CTB237, CTB238, CTB239, CTB240, CTB241, CTB242, CTB243, CTB244, CTB245, CTB246, CTB247, CTB248, CTB249, CTB250, CTB251, CTB252, CTB253, CTB254, CTB255, CTB256, CTB257, CTB258, CTB259, CTB260, CTB261, CTB262, CTB263, CTB264, CTB265, CTB266, CTB267, CTB268, CTB269, CTB270, CTB271, CTB272, CTB273, CTB274, CTB275, CTB276, CTB277, CTB278, CTB279, CTB280, CTB281, CTB282, CTB283, CTB284, CTB285, CTB286, CTB287, CTB288, CTB289, CTB290, CTB291, CTB292, CTB293, CTB294, CTB295, CTB296, CTB297, CTB298, CTB299, CTB300, CTB301, CTB302, CTB303, CTB304, CTB305, CTB306, CTB307, CTB308, CTB309, CTB310, CTB311, CTB312, CTB313, CTB314, CTB315, CTB316, CTB317, CTB318, CTB319, CTB320, CTB321, CTB322, CTB323, CTB324, CTB325, CTB326, CTB327, CTB328, CTB329, CTB330, CTB331, CTB332, CTB333, CTB334, CTB335, CTB336, CTB337, CTB338, CTB339, CTB340, CTB341, CTB342, CTB343, CTB344, CTB345, CTB346, CTB347, CTB348, CTB349, CTB350, CTB351, CTB352, CTB353, CTB354, CTB355, CTB356, CTB357, CTB358, CTB359, CTB360, CTB361, CTB362, CTB363, CTB364, CTB365, CTB366, CTB367, CTB368, CTB369, CTB370, CTB371, CTB372, CTB373, CTB374, CTB375, CTB376, CTB377, CTB378, CTB379, CTB380, CTB381, CTB382, CTB383, CTB384, CTB385, CTB386, CTB387, CTB388, CTB389, CTB390, CTB391, CTB392, CTB393, CTB394, CTB395, CTB396, CTB397, CTB398, CTB399, CTB400, CTB401, CTB402, CTB403, CTB404, CTB405, CTB406, CTB407, CTB408, CTB409, CTB410, CTB411, CTB412, CTB413, CTB414, CTB415, CTB416, CTB417, CTB418, CTB419, CTB420, CTB421, CTB422, CTB423, CTB424, CTB425, CTB426, CTB427, CTB428, CTB429, CTB430, CTB431, CTB432, CTB433, CTB434, CTB435, CTB436, CTB437, CTB438, CTB439, CTB440, CTB441, CTB442, CTB443, CTB444, CTB445, CTB446, CTB447, CTB448, CTB449, CTB450, CTB451, CTB452, CTB453, CTB454, CTB455, CTB456, CTB457, CTB458, CTB459, CTB460, CTB461, CTB462, CTB463, CTB464, CTB465, CTB466, CTB467, CTB468, CTB469, CTB470, CTB471, CTB472, CTB473, CTB474, CTB475, CTB476, CTB477, CTB478, CTB479, CTB480, CTB481, CTB482, CTB483, CTB484, CTB485, CTB486, CTB487, CTB488, CTB489, CTB490, CTB491, CTB492, CTB493, CTB494, CTB495, CTB496, CTB497, CTB498, CTB499, CTB500, CTB501, CTB502, CTB503, CTB504, CTB505, CTB506, CTB507, CTB508, CTB509, CTB510, CTB511, CTB512, CTB513, CTB514, CTB515, CTB516, CTB517, CTB518, CTB519, CTB520, CTB521, CTB522, CTB523, CTB524, CTB525, CTB526, CTB527, CTB528, CTB529, CTB530, CTB531, CTB532, CTB533, CTB534, CTB535, CTB536, CTB537, CTB538, CTB539, CTB540, CTB541, CTB542, CTB543, CTB544, CTB545, CTB546, CTB547, CTB548, CTB549, CTB550, CTB551, CTB552, CTB553, CTB554, CTB555, CTB556, CTB557, CTB558, CTB559, CTB560, CTB561, CTB562, CTB563, CTB564, CTB565, CTB566, CTB567, CTB568, CTB569, CTB570, CTB571, CTB572, CTB573, CTB574, CTB575, CTB576, CTB577, CTB578, CTB579, CTB580, CTB581, CTB582, CTB583, CTB584, CTB585, CTB586, CTB587, CTB588, CTB589, CTB590, CTB591, CTB592, CTB593, CTB594, CTB595, CTB596, CTB597, CTB598, CTB599, CTB600, CTB601, CTB602, CTB603, CTB604, CTB605, CTB606, CTB607, CTB608, CTB609, CTB610, CTB611, CTB612, CTB613, CTB614, CTB615, CTB616, CTB617, CTB618, CTB619, CTB620, CTB621, CTB622, CTB623, CTB624, CTB625, CTB626, CTB627, CTB628, CTB629, CTB630, CTB631, CTB632, CTB633, CTB634, CTB635, CTB636, CTB637, CTB638, CTB639, CTB640, CTB641, CTB642, CTB643, CTB644, CTB645, CTB646, CTB647, CTB648, CTB649, CTB650, CTB651, CTB652, CTB653, CTB654, CTB655, CTB656, CTB657, CTB658, CTB659, CTB660, CTB661, CTB662, CTB663, CTB664, CTB665, CTB666, CTB667, CTB668, CTB669, CTB670, CTB671, CTB672, CTB673, CTB674, CTB675, CTB676, CTB677, CTB678, CTB679, CTB680, CTB681, CTB682, CTB683, CTB684, CTB685, CTB686, CTB687, CTB688, CTB689, CTB690, CTB691, CTB692, CTB693, CTB694, CTB695, CTB696, CTB697, CTB698, CTB699, CTB700, CTB701, CTB702, CTB703, CTB704, CTB705, CTB706, CTB707, CTB708, CTB709, CTB710, CTB711, CTB712, CTB713, CTB714, CTB715, CTB716, CTB717, CTB718, CTB719, CTB720, CTB721, CTB722, CTB723, CTB724, CTB725, CTB726, CTB727, CTB728, CTB729, CTB730, CTB731, CTB732, CTB733, CTB734, CTB735, CTB736, CTB737, CTB738, CTB739, CTB740, CTB741, CTB742, CTB743, CTB744, CTB745, CTB746, CTB747, CTB748, CTB749, CTB750, CTB751, CTB752, CTB753, CTB754, CTB755, CTB756, CTB757, CTB758, CTB759, CTB760, CTB761, CTB762, CTB763, CTB764, CTB765, CTB766, CTB767, CTB768, CTB769, CTB770, CTB771, CTB772, CTB773, CTB774, CTB775, CTB776, CTB777, CTB778, CTB779, CTB780, CTB781, CTB782, CTB783, CTB784, CTB785, CTB786, CTB787, CTB788, CTB789, CTB790, CTB791, CTB792, CTB793, CTB794, CTB795, CTB796, CTB797, CTB798, CTB799, CTB800, CTB801, CTB802, CTB803, CTB804, CTB805, CTB806, CTB807, CTB808, CTB809, CTB810, CTB811, CTB812, CTB813, CTB814, CTB815, CTB816, CTB817, CTB818, CTB819, CTB820, CTB821, CTB822, CTB823, CTB824, CTB825, CTB826, CTB827, CTB828, CTB829, CTB830, CTB831, CTB832, CTB833, CTB834, CTB835, CTB836, CTB837, CTB838, CTB839, CTB840, CTB841, CTB842, CTB843, CTB844, CTB845, CTB846, CTB847, CTB848, CTB849, CTB850, CTB851, CTB852, CTB853, CTB854, CTB855, CTB856, CTB857, CTB858, CTB859, CTB860, CTB861, CTB862, CTB863, CTB864, CTB865, CTB866, CTB867, CTB868, CTB869, CTB870, CTB871, CTB872, CTB873, CTB874, CTB875, CTB876, CTB877, CTB878, CTB879, CTB880, CTB881, CTB882, CTB883, CTB884, CTB885, CTB886, CTB887, CTB888, CTB889, CTB890, CTB891, CTB892, CTB893, CTB894, CTB895, CTB896, CTB897, CTB898, CTB899, CTB900, CTB901, CTB902, CTB903, CTB904, CTB905, CTB906, CTB907, CTB908, CTB909, CTB910, CTB911, CTB912, CTB913, CTB914, CTB915, CTB916, CTB917, CTB918, CTB919, CTB920, CTB921, CTB922, CTB923, CTB924, CTB925, CTB926, CTB927, CTB928, CTB929, CTB930, CTB931, CTB932, CTB933, CTB934, CTB935, CTB936, CTB937, CTB938, CTB939, CTB940, CTB941, CTB942, CTB943, CTB944, CTB945, CTB946, CTB947, CTB948, CTB949, CTB950, CTB951, CTB952, CTB953, CTB954, CTB955, CTB956, CTB957, CTB958, CTB959, CTB960, CTB961, CTB962, CTB963, CTB964, CTB965, CTB966, CTB967, CTB968, CTB969, CTB970, CTB971, CTB972, CTB973, CTB974, CTB975, CTB976, CTB977, CTB978, CTB979, CTB980, CTB981, CTB982, CTB983, CTB984, CTB985, CTB986, CTB987, CTB988, CTB989, CTB990, CTB991, CTB992, CTB993, CTB994, CTB995, CTB996, CTB997, CTB998, CTB999, CTB1000
Transporters	SLC1A1, SLC1A3, SLC1A6, SLC1A4, SLC1A5, SLC7A8, SLC43A2, SLC6A15, SLC6A17, SLC6A19, SLC38A1, SLC38A2, SLC38A4, SLC38A5, SLC38A7, SLC38A10, SLC38A11, SLC7A2, SLC7A14, SLC7A11, SLC25A29, SLC2A1, SLC2A2, SLC2A3, SLC2A4, SLC2A5, SLC2A8, SLC2A9, SLC2A12, SLC35A4, SLC35A5, SLC50A1, SLC35A3, SLC35B4, SLC35D2, CLCN3, CLCN5, CLCN7, MFSD5, MAGT1, MGMT1, MRS2, NIPA2, NIPAL1, Sodium-independent sulfate anion transporter, SLC4A4, SLC20A1, SLC20A2, SLCO1C1, SLCO3A1, SLCO4C1, LMBRD1, SLC5A6, SLC19A3, SLC25A32, SLC52A2, SLC52A3, SLC5A1, SLC5A4, SLC5A10,

1
2
3
4

SLC5A2, SLC28A1, SLC5A3, APOA1, APOA2, APOB, Apolipoprotein A-IV, APOC2, APOC3, APOC4, APOD, APOE, APOM, APOO, SLC6A2, SLC6A3, SLC6A4, SLC6A8, SLC6A9, SLC6A12, SLC6A13, SLC10A2, SLC5A12, SLC16A1, SLC16A9, SLC16A13, SLC17A6, SLC17A7, SLC26A2, SLC29A3, SLC44A2, SLC44A3, SLC44A4, SLC44A5, SLC45A2, SLC46A2
